

Lithium Niobate Ridge Waveguides Fabricated by Wet Etching

H. Hu, R. Ricken, W. Sohler, and R. B. Wehrspohn

Abstract—The fabrication of LiNbO₃ ridge waveguides etched by a mixture of HF and HNO₃ using chromium (Cr) stripes as masks is reported. Smooth etched surfaces are obtained by adding some ethanol into the etchant. Under-etching is nearly avoided by annealing the sample with the Cr masks before the wet etching process. Low-loss monomode ridge guides with a height of up to 8 μm and a width between 4.5 and 7.0 μm are demonstrated. As an example, the propagation losses in a 6.5-μm-wide and 8-μm-high structure are 0.3 dB/cm for transverse-electric and 0.9 dB/cm for transverse-magnetic polarization, respectively, at 1.55-μm wavelength.

Index Terms—Etching, integrated optics, lithium compounds, losses, ridge waveguides.

I. INTRODUCTION

RI DGE waveguides are important basic structures of integrated optics. In comparison with conventional guides, ridge waveguides can reduce bending losses improving in this way the integration level of optical devices. Moreover, ridge guides reduce the size of optical modes enhancing the efficiency of nonlinear effects [1]. In electrooptical materials such as lithium niobate (LiNbO₃, LN) ridges can also reduce the half-wave voltage or length of modulators [2].

A variety of methods has been investigated in the last years to fabricate optical ridge guides in LN. Etching is the key step to achieve guiding in the horizontal direction, but it has to be compatible with the fabrication technique yielding guiding in the vertical direction. Plasma etching has been used after planar titanium (Ti)-indiffusion or proton exchange for waveguide formation [3], [4]. Ion beam etching has also been used after crystal ion slicing and wafer bonding [2]. Furthermore, ridge waveguides have been fabricated by precision diamond saw cutting after preparing a planar waveguide by gluing MgO:LN to LN, followed by grinding and polishing [1]. Moreover, wet etching of proton-exchanged LN structures followed by Ti-indiffusion has been reported [5]. Wet etching after oxygen-ion implantation was also used to define ridge waveguides after Ti-indiffusion [6]. Ridge waveguides could also be fabricated in Z-cut LN by chemical etching after spatially selective domain inversion in combination with various techniques yielding vertical guiding [7].

Another very simple possibility is to deposit first a metallic stripe as mask on the $-Z$ surface [e.g., made of chromium (Cr)],

Manuscript received September 6, 2006; revised December 13, 2006. The work of H. Hu was supported by an Alexander von Humboldt Foundation fellowship.

H. Hu, R. Ricken, and W. Sohler are with the Department of Physics, University of Paderborn, D-33098 Paderborn, Germany (e-mail: sol_hu@physik.upb.de; r.ricken@physik.upb.de; soehler@physik.upb.de).

R. B. Wehrspohn is with Fraunhofer Fraunhofer Institut für Mechanics of Materials, D-06120 Halle, Germany (e-mail: ralf.b.wehrspohn@iwmm.fraunhofer.de).

Digital Object Identifier 10.1109/LPT.2007.892886

followed by wet chemical etching. However, this process suffers from two drawbacks. The first one is considerable under-etching, i.e., etching under the mask. The second one is the enlarged roughness of the etched surface. In this letter, we report how under-etching can be significantly reduced by annealing. Moreover, we demonstrate that a smooth etched LN surface can be obtained by adding some ethanol into the HF–HNO₃ etchant. Using this technique, high-quality monomode LN ridge waveguides with a width between 4.5 and 7 μm and a height up to 8 μm have been fabricated. The propagation loss in 6.5-μm-wide and 8-μm-high ridges, e.g., can be as low as 0.3 dB/cm for the fundamental transverse electric (TE) and 0.9 dB/cm for the fundamental transverse magnetic (TM) mode measured at 1.55-μm wavelength.

II. FABRICATION

The LN ridge waveguides were fabricated in five steps.

- 1) *Planar waveguide fabrication*: A Ti film of 70-nm thickness was vacuum-deposited by e-beam evaporation on the $-Z$ surface of a LN substrate of 0.5-mm thickness. Subsequently, it was in-diffused at 1060 °C for 8.5 h in an argon (7.5 h) and oxygen (1 h) atmosphere, respectively. The resulting Ti concentration profile (c_{Ti}), calculated with known diffusion coefficients [8], corresponds to half a Gaussian distribution with a surface concentration of $0.97 \times 10^{21} \text{ cm}^{-3}$ and a depth [full-width at half-maximum (FWHM)] of 3.24 μm. As the increase of the extraordinary index of refraction (n_e) is proportional to the Ti-concentration, a Gaussian distribution results as well with a surface index of 2.1477 at 1.55-μm wavelength and the same depth is obtained. However, as the increase of the ordinary index of refraction (n_o) is proportional to $(c_{Ti})^{0.55}$ [9], the n_o profile can be approximated by half a Gaussian distribution as well with a surface index of 2.2163, but a larger depth of 4.38 μm.
- 2) *Cr mask fabrication*: After carefully cleaning the sample, a Cr film of 60-nm thickness was deposited by sputtering on the surface of the planar waveguide. Subsequently, 4- to 12-μm-wide Cr stripes were defined by optical contact lithography with an e-beam written mask and wet etching using a Cerium Sulfate solution. Finally, the remaining photoresist structure was removed by acetone.
- 3) *Annealing*: The sample was annealed at 300 °C for 3 h to improve the adhesion of the Cr film. Without annealing, serious under-etching was observed.
- 4) *Wet etching*: The sample was etched in a mixture of 60-ml HF and 39-ml HNO₃ with a concentration of 40% and 100%, respectively, for several hours at room temperature with stirring. The etch rate of $-Z$ -cut LN was about 0.8 μm/h at 22 °C. When ethanol was added to this etchant with a volume ratio of 1 : 7, the etch rate was reduced to

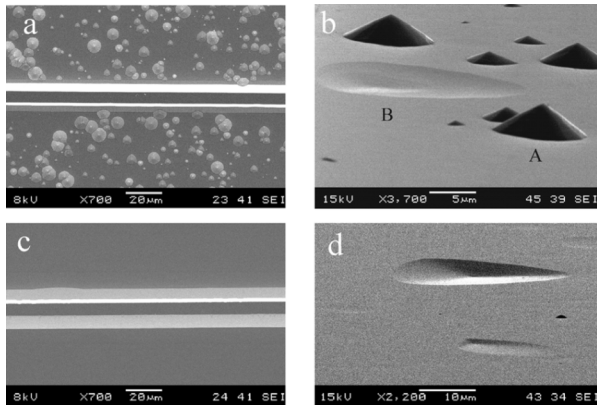


Fig. 1. SEM micrographs for comparison of two etched $-Z$ surfaces. (a) Top view of a surface with a ridge etched by HF-HNO₃ without ethanol; the bright stripes along both sides of the ridge are the etched walls. (b) Side view of two kinds of hillocks on the same surface as in (a) with higher magnification. (c) Top view of a surface with a ridge etched by HF-HNO₃ with ethanol; the bright stripes along both sides of the ridge are the etched walls. (d) Side view of hillocks on the same surface as in (c) with higher magnification; only a few hillocks are observed.

0.62 $\mu\text{m}/\text{h}$, but the smoothness of the etched surface was significantly improved. The etch rate of an X-cut surface was below 3 nm/h. The HF-HNO₃ mixture did virtually not attack the Cr stripes.

- 5) *Removal of Cr mask and end face polishing*: Using a cerium sulfate solution again, the Cr stripes were removed and the waveguide end faces were carefully polished using a SiO₂ suspension.

III. MORPHOLOGY OF SURFACES AND RIDGE STRUCTURES

Fig. 1 shows a comparison of the $-Z$ surfaces of undoped LN etched by HF-HNO₃ without and with ethanol. Fig. 1(a) is a top view of the LN surface etched without ethanol. The etch depth is about 7.5 μm . Fig. 1(b) is a side view of the sample surface, showing two types of hillocks, marked by A and B, respectively. The density of hillocks of type A is much higher than that of type B, and is affected by the intensity of stirring. Slow stirring generates a high density of hillocks. Fig. 1(c) is the LN surface etched by HF-HNO₃ with ethanol; the etching depth is about 9.6 μm . The surface is smoother than that shown in Fig. 1(a), but there are still some hillocks of type B on the surface, which are shown in Fig. 1(d). It seems that during the etching process small bubbles of hydrogen can be generated, which are adsorbed on the surface and impede further chemical etching. The result is a rough surface. Ethanol helps to avoid the bubble formation, yielding a much better surface quality, as shown in Fig. 1(c). An analogous explanation was reported in reference [10] for etching silicon.

Fig. 2 shows a top view of LN ridge waveguides fabricated without and with annealing after the Cr-mask definition. The waveguides are partially covered by the masking Cr stripe; its right hand part is peeled off to show the ridge underneath. Fig. 2(a) presents a ridge of about 5.9- μm height fabricated without annealing; it is about 3.3 μm smaller than the original Cr mask of 8.4- μm width. This difference depends on the intensity of stirring during etching; the faster the stirring the larger the difference becomes. Fig. 2(b) presents a ridge of 8- μm height fabricated after annealing the sample with a Cr

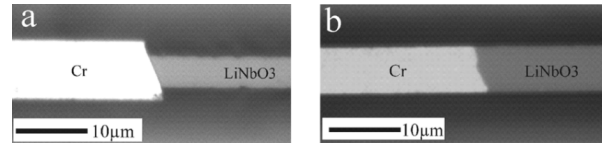


Fig. 2. Top view of ridge waveguides with partially removed Cr-mask under the optical microscope. (a) Fabricated by selective chemical etching without annealing after Cr-mask definition, and (b) with annealing.

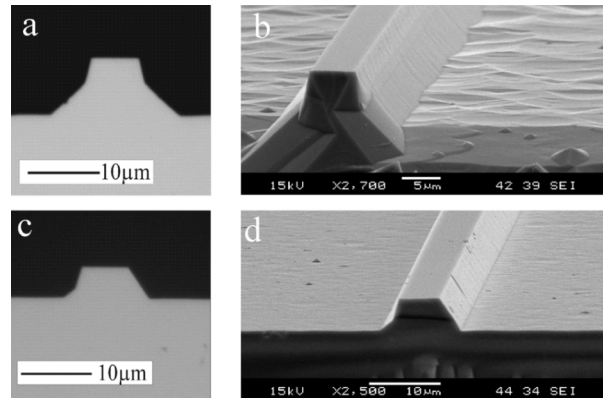


Fig. 3. (a) Optical micrograph of an end face of a Y-propagating ridge waveguide fabricated in Ti:LN. (b) SEM micrograph of etched wall and surface of Ti:LN. (c) Optical micrograph of an end face of a X-propagating ridge structure fabricated in undoped LN. (d) SEM micrograph of etched wall and surface of undoped LN.

mask of 6.5- μm width. It is evident that metallic mask and ridge have almost the same width; under-etching has been strongly reduced. The annealing process results in a tighter bonding of Cr and LN, which withstands the attack of the etchant. Otherwise, under-etching is observed.

Fig. 3(a) shows an end faces of a Y-propagating ridge waveguide fabricated with the annealing process. The etched ridge has walls of two different slopes; the reason is still unknown. Fig. 3(b) is a scanning electron micrograph (SEM) of an etched side wall and of the resulting surface of etched Ti:LN. The end face of the ridge guide shown in Fig. 3(b) was formed by wet etching. Fig. 3(c) shows the end face of a ridge, parallel to the crystallographic X-axis, in undoped LN. The two etched walls are asymmetric, which probably results from the different etching behavior of $+Y$ and $-Y$ surfaces [11]. A SEM micrograph of a cleaved ridge with etched wall and surfaces is shown in Fig. 3(d). The surface of etched undoped LN is much smoother than that of Ti:LN.

IV. OPTICAL WAVEGUIDE PROPERTIES

The propagation losses of the Y-propagating ridge waveguides with a length of 30 mm and a height of 8 μm were measured using the Fabry-Pérot resonance method at 1.55- μm wavelength [12]. In general, the losses are larger for TM- than for TE-polarization. Moreover, there is a tendency of decreasing loss as function of increasing waveguide width. For example, at 5.5- μm top width, the lowest TE-(TM-) propagation loss is 0.4 dB/cm (1.2 dB/cm), while at 6.5- μm top width, the lowest TE-(TM-) propagation loss is 0.3 dB/cm (0.9 dB/cm). The higher loss of the TM modes might be explained by the stronger confinement in the upper part of the ridge waveguide (see Fig. 4); therefore, the corresponding TM field strength is

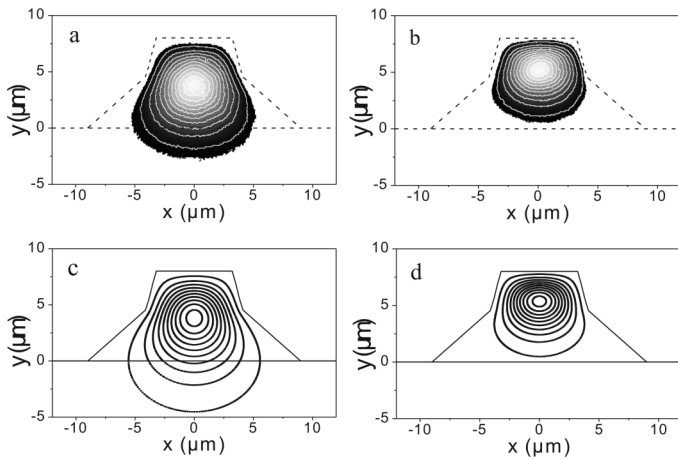


Fig. 4. Measured mode intensity distributions with contour lines in steps of 10% (upper graphs) and calculated distributions (lower graphs) in a Y-propagating ridge waveguide with a top width of $6.5 \mu\text{m}$. (a) TE mode; (b) TM mode. The shape of the ridge waveguides is indicated.

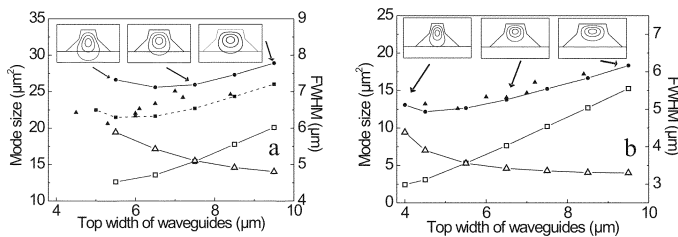


Fig. 5. (a) TE mode and (b) TM mode with the following: (\blacktriangle) measured mode size; (\bullet) calculated mode size; (\square) horizontal and (\triangle) vertical FWHM; (\blacksquare) calculated mode size with $+20\% \Delta n$; both plotted as function of the waveguide width at the top of the Y-propagating ridge guide.

higher at the etched sidewalls than for TE, resulting in stronger scattering by the residual roughness.

The polarization-dependent mode intensity profiles were measured at $1.55\text{-}\mu\text{m}$ wavelength using a standard setup magnifying the near field at the waveguide end face by a microscope objective. The results are shown in the upper row of Fig. 4. The Y-propagating ridge waveguides are monomode. It is evident that the TE mode has a larger extension than the TM mode due to the weaker guidance of the ordinary index profile in the depth.

Moreover, the corresponding intensity profiles have been calculated with a commercial software using the finite element method. The results are shown in the lower row of Fig. 4; they agree well with the measured mode distributions.

The mode size is an important parameter in particular for nonlinear optics applications. It was calculated and measured for a number of Y-propagating ridge waveguides of different width; the results are shown in Fig. 5. The mode size defined in this letter is the product of the FWHM of the mode intensity distribution in vertical and horizontal directions. The FWHM of the mode intensity in vertical direction is decreasing with increasing waveguide width, whereas the FWHM of the mode intensity in horizontal direction is increasing. Fig. 5(a) shows the TE mode size. It decreases as function of the waveguide width down to about $6.5 \mu\text{m}$, and increases at smaller widths when approaching cutoff. The calculated and measured TE mode sizes show a sim-

ilar dependence but with an offset. This difference might be due to the inaccuracy of the theoretical model describing the ordinary refractive index with its nonlinear dependence on the Ti concentration. By assuming a higher refractive index increase (20% increase), the mode sizes are recalculated and shown in Fig. 5(a) as well resulting in a somewhat better agreement of measured and calculated results. Fig. 5(b) shows the calculated and measured TM mode sizes, which agree well.

V. CONCLUSION

Three main results have been reported as follows: 1) A flat etched surface of pure LN is obtained by adding some amount of ethanol to the HF-HNO₃ etchant. 2) A Cr film can be used as mask in the wet etching process; appropriate annealing significantly reduces the underetching. 3) Monomode ridge waveguides of low propagation losses have been fabricated; as an example, they are 0.3 dB/cm for TE-, and 0.9 dB/cm for TM-polarization, respectively, in a guide of $6.5\text{-}\mu\text{m}$ width and $8\text{-}\mu\text{m}$ height at $1.55\text{-}\mu\text{m}$ wavelength.

ACKNOWLEDGMENT

The authors would like to thank B. Gesemann for initial finite-element-method calculations of the mode distributions. They also thank Dr. H. Suche, Dr. S. L. Schweizer, and Dr. H. Herrmann for helpful discussions.

REFERENCES

- [1] M. Iwai, T. Yoshino, S. Yamaguchi, M. Imaeda, N. Pavel, I. Shoji, and T. Taira, "High-power blue generation from a periodically poled MgO : LiNbO₃ ridge-type waveguide by frequency doubling of a diode end-pumped Nd : Y₃Al₅O₁₂ laser," *Appl. Phys. Lett.*, vol. 83, pp. 3659–3661, Nov. 2003.
- [2] P. Rabiei and W. H. Steier, "Lithium niobate ridge waveguides and modulators fabricated using smart guide," *Appl. Phys. Lett.*, vol. 86, 2005, Article 161115.
- [3] K. Noguchi, O. Mitomi, H. Miyazawa, and S. Seki, "A broadband Ti : LiNbO₃ optical modulator with a ridge structure," *J. Lightw. Technol.*, vol. 13, no. 6, pp. 1164–1168, Jun. 1995.
- [4] H. Hu, A. P. Milenin, R. B. Wehrspohn, H. Herrmann, and W. Sohler, "Plasma etching of proton-exchanged lithium niobate," *J. Vac. Sci. Technol. A*, vol. 24, pp. 1012–1015, Jul./Aug. 2006.
- [5] T.-L. Ting, L.-Y. Chen, and W.-S. Wang, "A novel wet-etching method using joint proton source in LiNbO₃," *IEEE Photon. Technol. Lett.*, vol. 18, no. 4, pp. 568–570, Feb. 15, 2006.
- [6] D. M. Gill, D. Jacobson, C. S. White, Y. Shi, W. J. Minford, and A. Harris, "Ridged LiNbO₃ modulators fabricated by a novel oxygen-ion implant/wet-etch technique," *J. Lightw. Technol.*, vol. 22, no. 3, pp. 887–894, Mar. 2004.
- [7] I. E. Barry, G. W. Ross, P. G. R. Smith, and R. W. Eason, "Ridge waveguides in lithium niobate fabricated by differential etching following spatially selective domain inversion," *Appl. Phys. Lett.*, vol. 74, pp. 1487–1488, Mar. 1999.
- [8] W. K. Burns, P. H. Klein, and E. J. West, "Ti diffusion in Ti : LiNbO₃ planar and channel optical waveguides," *J. Appl. Phys.*, vol. 50, pp. 6175–6182, Oct. 1979.
- [9] E. Strake, G. P. Bava, and I. Montrosset, "Guided modes of Ti : LiNbO₃ channel waveguides: A novel quasi-analytical technique in comparison with the scalar finite-element method," *J. Lightw. Technol.*, vol. 6, no. 6, pp. 1126–1135, Jun. 1988.
- [10] C. R. Yang, P. Y. Chen, Y. C. Chiou, and R. T. Lee, "Effects of mechanical agitation and surfactant additive on silicon anisotropic etching in alkaline KOH solution," *Sens. Actuators A*, vol. 119, pp. 263–270, 2005.
- [11] A. M. Prokhorov and Y. S. Kuz'minov, *Physics and Chemistry of Crystalline Lithium Niobate*. Bristol and New York: Adam Hilger, 1990, p. 120.
- [12] R. Regener and W. Sohler, "Loss in low-finesse Ti : LiNbO₃ optical waveguide resonators," *Appl. Phys. B*, vol. 36, pp. 143–147, 1985.